

JAERI-M  
9362

NUCLEAR EXCITATION BY ELECTRON  
TRANSITION (NEET) IN  $^{237}\text{Np}$  EXHIBITED  
BY K X-RAY SPECTRUM IN THE EC  
DECAY OF  $^{237}\text{Pu}$

February 1981

Atsushi SHINOHARA\*, Tadashi SAITO\*, Ryuichi ARAKAWA\*  
Kiyoteru OTOZAI\*, Hiroshi BABA, Kentaro HATA and  
Toshio SUZUKI

この報告書は、日本原子力研究所が JAERI-M レポートとして、不定期に刊行している研究報告書です。入手、複製などのお問い合わせは、日本原子力研究所技術情報部（茨城県那珂郡東海村）あて、お申しこしください。

JAERI-M reports, issued irregularly, describe the results of research works carried out in JAERI. Inquiries about the availability of reports and their reproduction should be addressed to Division of Technical Information, Japan Atomic Energy Research Institute, Tokai-mura, Naka-gun, Ibaraki-ken, Japan.

Nuclear Excitation by Electron Transition (NEET)  
in  $^{237}\text{Np}$  Exhibited by K X-ray Spectrum in the  
EC Decay of  $^{237}\text{Pu}$

Atsushi SHINOHARA\*, Tadashi SAITO\*, Ryuichi ARAKAWA\*  
Kiyoteru OTOZAI\*, Hiroshi BABA, Kentaro HATA and  
Toshio SUZUKI\*

Division of Radioisotope Production, JAERI

(Received January 31, 1981)

When a certain condition is satisfied, nuclear excitation by electron transition (NEET) becomes a possible deexcitation mode of atomic excitation due to an inner-shell vacancy, in addition to X-ray and Auger-electron emission. An attempt to detect NEET in  $^{237}\text{Np}$  following the EC decay of  $^{237}\text{Pu}$ , which preferentially decays to the ground state in  $^{237}\text{Np}$  by K-electron capture, was performed by examining the X-ray spectrum from  $^{237}\text{Pu}$ . The anomalies in the X-ray spectrum is expected to arise from perturbation leading to NEET. From the intensity ratio of the pair of perturbed  $K_{\alpha 1}$  X-ray peaks, the NEET probability for the 103-keV level in  $^{237}\text{Np}$  was deduced to have an upper limit of  $4 \times 10^{-3}$ .

Keywords: Nuclear Excitation, Electron Transition, KX-Ray Spectrum,  $^{237}\text{Pu}$ ,  $^{237}\text{Np}$ , EC Decay

---

+ Division of Chemistry, Tokai Research Establishment, JAERI

\* Osaka University

$^{237}\text{Pu}$  の EC 壊変に伴って放出される KX 線スペクトル中に  
認められる  $^{237}\text{Np}$  の電子遷移による核励起 (NEET)

日本原子力研究所アイソトープ事業部製造部

篠原 厚\*・斉藤 直\*・荒川隆一\*・音在清輝\*

馬場 宏・畑健太郎・鈴木敏夫<sup>+</sup>

(1981 年 1 月 31 日受理)

内殻イオン化による原子励起は、X線放射やオージェ電子放出により失活するが、原子核との間にある条件を満たすと、「電子遷移による核励起」(NEET)による失活が可能となる。本報告では、 $^{237}\text{Pu}$ の電子捕獲崩壊時に、娘核種の $^{237}\text{Np}$ においてNEETが起こり得る状態が出現することに着目し、その $^{237}\text{Np}$ におけるNEETの検出を試みた。検出は、NEETを引き起こす摂動の結果現われるサテライトX線のうち、 $K_{\alpha 1}$  X線のサテライト対を調べることにより行った。その結果、NEET確率の上限値として、 $4 \times 10^{-3}$ の値を得た。

---

+ 東海研究所原子炉化学部

\* 大阪大学

## Contents

1. Introduction	.....	1
2. Experimental		
2.1. SOURCE PREPARATION	.....	4
2.2. MEASUREMENT OF X-RAY SPECTRUM	.....	5
3. Analysis		
3.1. GENERAL	.....	7
3.2. ANALYSIS OF THE 103-keV PEAK	.....	9
3.3. ESTIMATE OF NEET- $\gamma$ , NUCLEAR- $\gamma$ AND (60-keV $\gamma$ + 43-keV $\gamma$ ) SUM PEAK	.....	10
3.4. ESTIMATE OF ( $K_{\alpha 1}$ + ( $L_{\ell}$ -Ge)) SUM PEAK	.....	11
3.5. DEDUCTION OF "NEET-X"	.....	13
4. Theory		
4.1. PRINCIPLE OF NEET	.....	14
4.2. SATELLITE X-RAYS IN THE NEET PROCESS	.....	16
5. Results and Discussion	.....	19
References	.....	25

## 目 次

1. まえがき	1
2. 実 験	
2.1 測定線源の調製	4
2.2 X線スペクトルの測定	5
3. 解 析	
3.1 概 論	7
3.2 103 -KeV ピークの解析	9
3.3 NEET- $\gamma$ , NUCLEAR- $\gamma$ , 及び (60 -KeV $\gamma$ 線+43 -KeV $\gamma$ 線) サムピーク強度の概算	10
3.4 (K $\alpha_1$ + (L1-Ge)) サムピーク強度の概算	11
3.5 "NEET-X" の解析強度	13
4. 理 論	
4.1 NEETの原理	14
4.2 NEET過程におけるサテライトX線	16
5. 結果及び考察	19
参考文献	25

## 1. Introduction

Ionization of an atomic inner shell provokes an electron transition from an outer shell to the vacated one. The energy is then dissipated in the form of the emission of characteristic X-rays or Auger electrons. Morita<sup>1)</sup> has proposed an additional deexcitation mode involving nuclear excitation instead of those emission modes. This process, named nuclear excitation by electron transition (in short, NEET), will take place if the following NEET conditions are satisfied: (i) Both nuclear and electronic transitions are of approximately the equal energy. (ii) They have a common multipolarity. The first experimental evidence of this process was obtained by Otozai et al.<sup>2,3)</sup>. They bombarded osmium metal with electrons to ionize the atomic K shell and succeeded in detecting the radioactivity of  $^{189m}\text{Os}$  induced via NEET.

The electron hole leading to NEET can be produced in the radioactive decay such as electron capture (EC) decay or internal conversion process, in addition to the bombardment with electrons and the irradiation with photons. For instance, if a daughter nuclide in the EC decay fulfills the NEET conditions, NEET will take place automatically following the decay of the parent nuclide. If such NEET process following the radioactive decay takes place to a considerable degree, it becomes indispensable both in the decay process and in the

decay scheme. Furthermore, the method applying this process is favorable for identifying the NEET phenomenon, since the competitive process such as the Coulomb excitation or the  $\gamma$ -ray resonance absorption as a consequence of the use of electrons or photons, respectively, need not be taken into account.

As Fig. 1 shows, the nuclear excitation,  $N$ , of a 102.95-keV level in  $^{237}\text{Np}$  and the electronic transition,  $A$ , between the K shell (118.680 keV) and the  $L_3$  subshell (17.608 keV) have very close transition energies and a common multipolarity  $E1$  of the lowest  $\ell$  value; namely, they satisfy the NEET conditions. Furthermore,  $^{237}\text{Pu}$  decays to the ground state in  $^{237}\text{Np}$  by K-electron capture with a large branching ratio. Therefore, NEET is expected to occur favorably in the EC decay of  $^{237}\text{Pu}$ . In this study, we attempted to detect NEET in  $^{237}\text{Np}$  following the EC decay of  $^{237}\text{Pu}$  and to obtain the information on NEET of  $E1$ , in addition to NEET of  $E2$  for the case of  $^{189}\text{Os}$ .

The nuclear excitation of the 103-keV level by the NEET process cannot be distinguished from direct feeding of  $^{237}\text{Pu}$  to the same level. However, the occurrence of NEET is detectable in some anomalies appearing in the X-ray spectrum from  $^{237}\text{Pu}$ . The NEET theory<sup>1,4)</sup> predicts that X-rays split into a pair of satellites as a consequence of perturbation in the resultant system of the nuclear and electronic states.



They are emitted in connection with two electronic transitions, one to the K shell with the nucleus in the ground state and the other to the  $L_3$  subshell with the nucleus in the 103-keV excited state. In the case of the L X-rays following the disappearance of the  $L_3$  vacancies, such as the L series of  $\alpha_{1,2}$ ,  $\beta_{2,5,6,7,15}$ ,  $\ell$ ,  $s$ ,  $t$  and  $u$ , their two weak satellites should coexist with the normal L X-rays emitted in the non-NEET states. Because of such complexity of the L X-rays, it was hard to detect those satellites.<sup>5)</sup>

On the other hand, perturbed K X-rays consist of a pair of the respective satellites. One of them is similar in energy and in intensity to the unperturbed X-ray, while the other of weaker intensity has a higher energy by approximately  $|\Delta|$  than the former when the level repulsion due to perturbation,  $\delta$ , is inappreciable as found in Ref.<sup>5)</sup>. Here  $\Delta$  is the energy difference between the nuclear and electronic transitions. Among the respective satellites of K X-rays, the satellites of  $K_{\alpha 1}$  X-ray were aimed at to investigate NEET. The weaker satellite of the  $K_{\alpha 1}$  X-ray will lie near 103 keV and may be detectable in the  $K_{\alpha 1}$  X-ray spectrum following the EC decay of  $^{237}\text{Pu}$ . Some quantitative information on NEET in  $^{237}\text{Np}$  will be obtained from the observed intensity ratio of the satellite pair.

## 2. Experimental

### 2.1. SOURCE PREPARATION

Besides the source of  $^{237}\text{Pu}$  for use in detection of the satellite X-rays, the sources of  $^{237}\text{U}$  and  $^{241}\text{Am}$ , which decay to the same daughter nuclide  $^{237}\text{Np}$  by  $\beta^-$  and  $\alpha$  decay, respectively, were prepared. Here  $^{237}\text{U}$  was used to take the unperturbed standard X-ray spectrum for comparison with the perturbed one from  $^{237}\text{Pu}$ , since  $^{237}\text{U}$  rarely decays to the state satisfying the NEET conditions in  $^{237}\text{Np}$ . Also,  $^{241}\text{Am}$  was used to determine the ratio of  $\gamma$ -rays which was necessary for the analysis of the satellite X-rays.

The activity of  $^{237}\text{Pu}$  was produced by the  $^{238}\text{U}(^3\text{He},4n)$  reaction as described elsewhere.<sup>6)</sup> A thick target of natural uranium metal was bombarded with 38-MeV  $^3\text{He}$  beam from the cyclotron at the Institute of Physical and Chemical Research. The irradiated uranium was dissolved in conc.  $\text{HNO}_3$ . The Pu fraction was isolated according to an ion-exchange scheme developed by Natsume et al.<sup>7)</sup> The eluate was dropped on a Mylar film and dried up by an infrared lamp. This sample was assayed to  $\alpha$ -ray spectrometry and found to contain small amounts of  $^{236}\text{Pu}$  and  $^{238}\text{Pu}$ . These contaminants, however, being  $\alpha$ -emitters with half-lives of 2.85 y and 87.75 y, respectively, produce negligible interference on the K X-ray region of Np.

The  $^{237}\text{U}$  source was also prepared by the chemical separation from the Pu solution which had been purified from spent nuclear fuel. Although thus prepared source contained other isotopes, these contaminants did not disturb the X-ray spectrum of  $^{237}\text{U}$ , because of their extremely low radioactivities.

The  $^{241}\text{Am}$  sample was supplied as well as  $^{237}\text{U}$  by the Nuclear Chemistry Laboratory of JAERI. The  $^{241}\text{Am}$  was mono-isotopic, since it was prepared by milking the Pu solution which had been separated from spent nuclear fuel and contained  $^{241}\text{Pu}$ , the only  $\beta^-$ -emitting isotope with long life.

## 2.2. MEASUREMENT OF X-RAY SPECTRUM

The photon spectra of  $^{237}\text{Pu}$ ,  $^{237}\text{U}$  and  $^{241}\text{Am}$  were taken with two low-energy photon spectrometer systems. One system consisted of a hyperpure Ge detector with resolution of 510 eV at 122 keV connected with standard electronic equipments. The output pulses from a linear amplifier were fed to a 1 kch pulse height analyzer (MCA) through a biased amplifier. The K and L X-rays from  $^{237}\text{Pu}$ ,  $^{237}\text{U}$  and  $^{241}\text{Am}$  were measured with various electronic settings in the separate runs. The  $\gamma$ -ray spectrum of  $^{241}\text{Am}$  was also taken with this system. Each source was placed at a distance of 5 mm from the Be window of the detector. The data acquisition was continued for 1000–7000 min. The other system consisting of a Ge(Li) detector

with a 4 kch MCA was also used. Decay of  $^{237}\text{Pu}$  was followed for 20 months with this system.

The detection efficiency and the Ge  $K_{\alpha}$ -escape ratio as a function of energy were determined for the former detector system, since they were needed in the analysis of the satellite X-rays. The detection efficiency was calibrated by using the gamma reference sources supplied by TRC Amersham. The escape ratios were obtained by measuring the intensities of the photopeaks and their escape peaks for various X- and  $\gamma$ -rays. As found in Fig. 2, the obtained escape ratio function agreed well with that calculated by Fioratti and Piermattei<sup>8)</sup>.

These photon spectra were analyzed by using the BOB73 and BOB75  $\gamma$ -ray spectrum analyzing codes<sup>9-11)</sup>. The region of interest, the neighborhood of 103 keV, was inspected manually as described in the next chapter. The typical photon spectra of  $^{237}\text{Pu}$ ,  $^{237}\text{U}$  and  $^{241}\text{Am}$  are shown in Figs. 3-5.

### 3. Analysis

#### 3.1. GENERAL

Among the respective satellite lines of K X-rays of Np, we aimed at the weaker satellite of the  $K_{\alpha 1}$  X-ray, designated as "NEET-X" in the text, because of its simplicity in the analysis. Detection of "NEET-X" requires the information on  $\delta$ , since "NEET-X" lies at higher energy by  $|\Delta + 2\delta|$  than its participant satellite which is similar in energy to the unperturbed  $K_{\alpha 1}$  X-ray. Although the energy shift seems to be inappreciable as found by Otozai et al.<sup>5)</sup>, this can be further confirmed by comparing the energies of perturbed X-rays with those of unperturbed ones. Then, the X-rays from  $^{237}\text{U}$  were used as the unperturbed standard X-rays for comparison with the perturbed ones. In  $^{237}\text{U}$ , the K X-rays are emitted mainly in the internal conversion process from a 281-keV level or a 268-keV level to the lower excited ones and rarely in that to the ground level, namely, in the state satisfying the NEET conditions in  $^{237}\text{Np}$ . Therefore, the Np K X-rays from  $^{237}\text{U}$  are considered to consist almost of the ordinary unperturbed X-rays (unperturbed component: 99%, perturbed one: 1%). As a consequence of the comparative measurement between the respective K X-rays from  $^{237}\text{Pu}$  and  $^{237}\text{U}$ , they were found to have the equal energies within the experimental errors. It was thus confirmed that the value of  $|\delta|$  was extremely small compared

with  $|\Delta|$  and consequently "NEET-X" should lie at a higher energy by about  $|\Delta|$ , near 102.95 keV.

As will be described later, some information on NEET can be deduced from the intensity ratio of a pair of satellites of the  $K_{\alpha 1}$  X-ray. Quantitative analysis of the "NEET-X" is, however, not easy because of the following reasons. First, the "NEET-X" peak lying at 102.95 keV coincides accidentally with other several peaks. Secondly, the 103-keV peak with weak intensity lies in the outskirts of the high-energy side of the intense  $K_{\alpha 1}$  peak of 101.072 keV. Fig. 6 shows the typical photon spectrum in the neighborhood of "NEET-X".

The components of the 103-keV peak are as follows:

- (1) "NEET-X": The weaker satellite of the  $K_{\alpha 1}$  X-ray, due to perturbation, the energy of which we may consider to be practically equal to that of the relevant nuclear transition, 102.95 keV.
- (2) NEET- $\gamma$ : A  $\gamma$ -ray being emitted when a nuclear transition occurs to the ground state from the 103-keV level excited by NEET.
- (3) Nuclear- $\gamma$ : A  $\gamma$ -ray with energy of 103 keV except the component (2). This is emitted when the 103-keV state in  $^{237}\text{Np}$ , fed by  $^{237}\text{Pu}$  in an ordinary branching, decays to the ground state directly.
- (4) (60-keV  $\gamma$  + 43-keV  $\gamma$ ) sum peak: A sum peak of the 60-keV and 43-keV  $\gamma$ -rays, both of which may be emitted in cascade

in the deexcitation of 103-keV state with considerable probability.

(5) ( $K_{\alpha 1} + (L_{\ell} - \text{Ge})$ ) sum peak: A sum peak of the Np  $K_{\alpha 1}$  X-ray peak and the Ge-escape peak of the  $L_{\ell}$  X-ray, the energy of which falls approximately on 103 keV.

In order to obtain the intensity of "NEET-X", we analyzed the 103-keV peak and estimated the intensity of each component except "NEET-X" with the theoretical and experimental methods, as described below.

### 3.2. ANALYSIS OF THE 103-keV PEAK

The 103-keV peak was failed to be recognized by the automatic peak-search routine of the BOB code because of its extremely low intensity relative to the intense neighboring  $K_{\alpha 1}$  peak. Then, the region of interest was inspected manually as follows.

First, since part of the Ge-escape peaks of  $K_{\beta}$  X-rays were located in the region in question, continuous background due to the Ge-escape effect was subtracted from the counts in the region by using the escape ratio which had been found experimentally to be about  $1 \times 10^{-3}$ .

Next, the intensity of the 103-keV peak,  $I_{tot}^{103}$ , was obtained by subtracting the smooth baseline which was interpolated by a polynomial function fitted to the observed counts except

the peak region assumed to be equivalent to the full width at tenth maximum of the peak. This procedure is based on the assumption that the region used for the polynomial fitting consists of only the smooth tailing of the intense  $K_{\alpha 1}$  peak. The polynomial fitting was carried out by the least squares method with an ACOS computer. As the consequence of it, the fifth order polynomial gave a best fit to the observed counts, and its reduced  $\chi^2$  value was 0.97 for 26 degrees of freedom. The region used for the analysis and the extracted 103-keV peak are shown in Fig. 7. The error attached to each count was estimated from the statistical errors in the measurement and in the least squares fit. Finally, the value of  $I_{tot}^{103}$  was obtained by adding all the extracted counts in the peak region.

### 3.3. ESTIMATE OF NEET- $\gamma$ , NUCLEAR- $\gamma$ , AND (60-keV $\gamma$ + 43-keV $\gamma$ ) SUM PEAK

It is very difficult to distinguish NEET- $\gamma$  from nuclear- $\gamma$ , since both  $\gamma$ -rays originate in the same 103-keV level. As shown in Fig. 1, the 103-keV level feeds to the 33-keV and the 60-keV levels as well as the ground one. Therefore, if their relative branching ratios are known, the total intensity  $I_{\gamma}^{103}$  of NEET- $\gamma$ , nuclear- $\gamma$ , and (60-keV  $\gamma$  + 43-keV  $\gamma$ ) sum peak can be derived from the intensity of the 43-keV or 70-keV  $\gamma$ -ray. In this analysis, the 43-keV  $\gamma$ -ray was used because the 70-keV



$\gamma$ -ray was not observed.

The intensity ratio of the 103-keV  $\gamma$ -ray to the 43-keV  $\gamma$ -ray was determined from the  $\gamma$ -ray spectrum of  $^{241}\text{Am}$ . The ratio was determined as  $I_{\gamma}^{103}/I_{\gamma}^{43} = 0.204 \pm 0.006$ . Since the measurements of  $^{241}\text{Am}$  and  $^{237}\text{Pu}$  were performed under the same conditions, this value includes the effects of the detection efficiency and the sum peak.

In determining  $I_{\gamma}^{43}$  of  $^{237}\text{Pu}$ , the contribution of a 43.48-keV  $\gamma$ -ray of  $^{238}\text{Pu}$ , which is one of the impurities, has to be taken into account.  $I_{\gamma}^{43}$  was obtained by analyzing the decay of two components,  $^{237}\text{Pu}$  ( $t_{1/2} = 45.4$  d) and  $^{238}\text{Pu}$  ( $t_{1/2} = 87.75$  y), with the aid of the CLSQ code<sup>12)</sup>. Finally, the value of  $I_{\gamma}^{103}$  of  $^{237}\text{Pu}$  was deduced from the ones of  $I_{\gamma}^{43}$  and  $I_{\gamma}^{103}/I_{\gamma}^{43}$ .

### 3.4. ESTIMATE OF $(K_{\alpha 1} + (L_{\ell} - \text{Ge}))$ SUM PEAK

In the X-ray spectrum shown in Fig. 6, the complex peaks at 103–105 keV can be explained by sum peaks of K X-ray peaks and the Ge-escape peaks of L X-rays and by those of  $K_{\alpha 1}$  X-ray peak and M X-ray peaks. These sum peaks arised as an inevitable consequence of the measurements with a large geometric efficiency. The complex peaks are considered to consist of five components containing the  $(K_{\alpha 1} + (L_{\ell} - \text{Ge}))$  sum peak, as seen in Table 1 and Fig. 6. Here, sum peaks of L X-ray

peaks and the Ge-escape peaks of K X-rays were neglected because of their extremely low escape ratios.

Then, the intensity of relevant sum peak,  $I_{sum}^{103}$ , was estimated with the following procedure. At first, the intensities per decay of these components were calculated theoretically by using the data of Refs.<sup>13,14)</sup> and the detection efficiency, the escape ratios, and the geometric efficiency in this experiment. The procedure of this calculation was based on the assumption that these sum peaks resulted from the following X-rays: (i) the K X-ray and L or M X-ray emitted in cascade, (ii) the K X-ray following the EC decay and the L or M X-ray following the internal conversion process when  $^{237}\text{Pu}$  decays to an excited state in  $^{237}\text{Np}$  by K-electron capture. Subsequently, the estimates of sum peaks which would be detected in this experiment were derived from the theoretical intensities of these sum peaks and the observed ones of  $K_{\alpha 1}$  and  $K_{\alpha 2}$  X-rays. These values and the observed ones are listed in Table 1. The estimated intensities are slightly larger than the observed ones, but explain well the peak group at 103–105 keV. Finally, the value of  $I_{sum}^{103}$  was deduced from the estimated intensity ratio and the observed intensities of other components, as given in Table 1. Their uncertainties were incapable of being estimated because of the ignorance of errors for many factors in the calculation.

## 3.5. DEDUCTION OF "NEET-X"

As described above, the intensity of the 103-keV peak and that of each component except "NEET-X" were obtained. Consequently, the intensity of the "NEET-X",  $I_X^{103}$ , can be deduced as

$$I_X^{103} = I_{tot}^{103} - (I_\gamma^{103} + I_{sum}^{103}).$$

These results are summarized in Table 2. The error of  $I_X^{103}$  is considered to be a little larger than the tabulated value because of the ignorance of the error of  $I_{sum}^{103}$ . The intensity ratio of the "NEET-X" to the  $K_{\alpha 1}$  X-ray then becomes

$$Q = (I_X^{103}/I_{K\alpha 1}) = (4 \pm 9) \times 10^{-5}.$$

The result obtained is obviously insufficient to show the evidence of NEET in  $^{237}\text{Np}$ , but will give an upper limit of the NEET probability.

## 4. Theory

### 4.1. PRINCIPLE OF NEET

The principle of NEET is illustrated in Fig. 8 and briefly described below according to Refs.<sup>1,3)</sup>. In Fig. 8, the wave function  $\Psi_1$  is the unperturbed system consisting of the initial electron hole state  $\phi_1$  and the nuclear ground state  $\psi_1$ , and  $\Psi_2$  is that of the next electron hole state  $\phi_2$  and the nuclear excited state  $\psi_2$ . The energies for the states  $\phi_1$ ,  $\phi_2$ ,  $\psi_1$ , and  $\psi_2$  are designated with  $E_1$ ,  $E_2$ , 0, and  $E_N$ , respectively.

The excitation energy difference,  $\Delta$ , is also defined as

$$\Delta = (E_1 - E_2) - E_N.$$

If the electronic transition,  $A$ , and the nuclear excitation,  $N$ , have a common multipolarity and  $|\Delta|$  is very small, the states  $\Psi_1$  and  $\Psi_2$  are no longer the eigenstates of the resulting system. From the standard perturbation theory, the true eigenstates  $\Phi_1$  and  $\Phi_2$  are expressed by

$$\Phi_1 = \Psi_1 \cos \theta + \Psi_2 \sin \theta,$$

$$\Phi_2 = -\Psi_1 \sin \theta + \Psi_2 \cos \theta.$$

Here,  $\theta$  is the mixing angle and defined as,

$$\cos \theta \cdot \sin \theta = \frac{(\Psi_2 | H' | \Psi_1)}{E(\Phi_1) - E(\Phi_2)},$$

where  $E(\Phi_1)$  and  $E(\Phi_2)$  refer to the energies for the states  $\Phi_1$

and  $\phi_2$ , respectively, and  $H'$  is a perturbation operator. For small  $\theta$  the above equation becomes approximately

$$\tan\theta = E'/\Delta, \quad (1)$$

where

$$E' = (\Psi_2 | H' | \Psi_1). \quad (2)$$

Here,  $E'$  is the electromagnetic interaction energy between the orbital electron and the nucleus.

When the state  $\Psi_1$  is created, the states  $\phi_1$  and  $\phi_2$  are produced with the probabilities of  $\cos^2\theta$  and  $\sin^2\theta$ , respectively. Decay of the component  $\psi_2\phi_2$  of the state  $\phi_1$  or  $\phi_2$  to one of the states  $\psi_2\phi_i$  ( $i=3,4,\dots$ ) provokes the nuclear excitation. The probability of producing the nuclear excited state  $\psi_2$  from the state  $\Psi_1$ , referred as the NEET probability,  $P$ , is therefore expressed by

$$P = \sum_{i=3} [(\lambda_{2i} \cos^2\theta / \Lambda_{\phi_2}) \sin^2\theta + (\lambda_{2i} \sin^2\theta / \Lambda_{\phi_1}) \cos^2\theta].$$

Here,  $\Lambda$ 's are the total decay constants and obtained from

$$\begin{aligned} \Lambda_{\phi_1} &= \Lambda_1 \cos^2\theta + \Lambda_2 \sin^2\theta, \\ \Lambda_{\phi_2} &= \Lambda_1 \sin^2\theta + \Lambda_2 \cos^2\theta, \end{aligned} \quad (3)$$

with

$$\Lambda_1 = \sum_{i=2} \lambda_{1i}, \quad \Lambda_2 = \sum_{j=3} \lambda_{2j},$$

where  $\lambda_{if}$  is the decay constant for the electronic transition

$\phi_i \rightarrow \phi_f$ . Therefore, for small  $\theta$  the NEET probability  $P$  becomes approximately

$$P = (1 + \Lambda_2/\Lambda_1)\tan^2\theta. \quad (4)$$

From the energy conservation, the energy repulsion of the resulting system due to perturbation is also expressed by

$$\delta = E'^2/\Delta. \quad (5)$$

#### 4.2. SATELLITE X-RAYS IN THE NEET PROCESS

The X-ray spectrum becomes complex if an appreciable amount of NEET takes place as shown in Fig. 8. Two states  $\phi_1$  and  $\phi_2$  decay to  $\psi_1\phi_2$ ,  $\psi_1\phi_3$ ,... in the nuclear ground state and to  $\psi_2\phi_3$ ,  $\psi_2\phi_4$ ,... in the nuclear excited state. Therefore, one can expect to observe two splitted X-rays  $C$  and  $C^*$  (cf. Fig. 8) instead of the unperturbed X-ray  $C^0$ , and  $D$  and  $D^*$  for  $D^0$  X-ray. The X-ray spectrum expected for these transitions is illustrated in Fig. 9. Some formulas for the  $C$  and  $C^*$  transitions, which are needed in extracting the NEET probability and its related quantities from the experimental results, are derived here according to the description of these satellite X-rays by Otozai<sup>4)</sup>.

The energies for the  $C$  and  $C^*$  transitions are  $(E_1 - E_2 + \delta)$  and  $(E_1 - E_2 - \delta - \Delta)$ , respectively. However, we may consider

that, since  $\delta$  is thought to be very small, the X-ray emitted in the  $C$  transition has approximately the unperturbed X-ray energy,  $E_1 - E_2$ , and the one emitted in the  $C^*$  transition has a higher energy by about  $|\Delta|$  than it because the sign of  $\Delta$  is negative for  $^{237}\text{Np}$ .

Next, the probability for the  $C$  transition per appearance of  $\Psi_1$  state,  $P_C$ , is expressed by

$$P_C = (\lambda_{12} \cos^2 \theta / \Lambda_{\phi 1}) \cos^2 \theta, \quad (6)$$

and for the  $C^*$  transition,

$$P_{C^*} = (\lambda_{12} \sin^2 \theta / \Lambda_{\phi 2}) \sin^2 \theta. \quad (7)$$

In the case that the NEET conditions are satisfied automatically in the EC decay, such as in the present experiment, we must take into account the  $C^o$  transition occurring in the state which does not satisfy the NEET conditions. When the state satisfying the NEET conditions,  $\Psi_1$ , is produced with the probability  $B(\Psi_1)$  in the EC decay, the probabilities for the  $C$  and  $C^*$  transitions per disintegration of  $^{237}\text{Pu}$ ,  $B(C)$  and  $B(C^*)$ , are expressed by

$$B(C) = B(\Psi_1) P_C, \quad (8)$$

$$B(C^*) = B(\Psi_1) P_{C^*}. \quad (9)$$

The probability for the  $C^o$  transition per disintegration,  $B(C^o)$ , is also given as

$$B(C^o) = [B(\phi_1) - B(\psi_1)]\lambda_{12}/\Lambda_1, \quad (10)$$

where  $B(\phi_1)$  is the probability of producing the electronic state  $\phi_1$  per disintegration. Then the intensity ratio of the weaker satellite X-ray (for the  $C^*$  transition) to the participant satellite X-ray (for both  $C$  and  $C^o$  transitions since both transitions have almost equal energies),  $Q$ , is expressed by

$$Q = \frac{B(C^*)}{B(C^o) + B(C)}.$$

Combining Eqs. (6)–(10) with the above equation, one obtains

$$Q = \frac{B(\psi_1)\sin^4\theta/\Lambda_{\phi 2}}{B(\psi_1)\cos^4\theta/\Lambda_{\phi 1} + [B(\phi_1) - B(\psi_1)]/\Lambda_1}.$$

Using the relations,  $\Lambda_{\phi 1} \approx \Lambda_1$  and  $\Lambda_{\phi 2} \approx \Lambda_2$ , obtained from Eq. (3) for small  $\theta$ , one can write the above equation in the form

$$Q = \frac{B(\psi_1)\sin^4\theta}{B(\psi_1)\cos^4\theta + [B(\phi_1) - B(\psi_1)]} \frac{\Lambda_1}{\Lambda_2}. \quad (11)$$

Using the above equation and the experimental value of  $Q$ , we can obtain the mixing angle  $\theta$ , from which the values of  $P$ ,  $E'$ , and such are derived.



## 5. Results and Discussion

The information on NEET, e.g., the NEET probability  $P$  and the electromagnetic interaction energy  $E'$  can be obtained from the experimental value of  $Q$  and Eqs. (1), (4), and (11). The obtained value of  $I_X^{103}$  is, however, apparently lower than the critical level, which was defined in Ref.<sup>15)</sup>, in this experiment, so that the decision, "not detected," should be reported, and an upper limit of  $I_X^{103}$  should be given instead; namely,  $(5 + u \times 11) \times 10^{-4}$  cps. The  $Q$ 's was then obtained as  $(4 + u \times 9) \times 10^{-5}$ . Here  $u$  refers to the one-sided confidence interval. Then, we used  $Q < 1.3 \times 10^{-4}$  as the upper limit of  $Q$  in  $u = 1$  (84% one-sided confidence level) in order to estimate the upper limits of  $P$  and  $E'$ .

In  $^{237}\text{Np}$ , the states  $\phi_1$  and  $\phi_2$  correspond to the K-hole state and the  $L_3$ -hole state, respectively. The energies are  $E_K = 118.680$  keV,  $E_{L_3} = 17.608$  keV, and  $E_N = 102.95$  keV as shown in Fig. 1. Also  $\Delta$  is  $-1.88$  keV. The value of  $\Lambda_2/\Lambda_1$ , namely,  $\Lambda_{L_3}/\Lambda_K$ , is equal to that of  $\Gamma(L_3)/\Gamma(K)$ , where  $\Gamma(K)$  and  $\Gamma(L_3)$  are the level widths of the K shell and the  $L_3$  subshell, respectively.  $\Gamma(L_3)/\Gamma(K)$  was derived from the X-ray emission rates calculated by Scofield<sup>19)</sup> and the fluorescence yields obtained by Ahmad<sup>17)</sup> and Fink and Rao<sup>18)</sup>, and consequently  $\Lambda_{L_3}/\Lambda_K = 0.079$  was obtained. The values of  $B(\phi_K)$  and  $B(\psi_1)$  were also calculated with the nuclear data and the appendix 22

in Ref.<sup>14)</sup>, and obtained as  $B(\phi_K) = 0.497$  and  $B(\psi_1) = 0.440$ .

Resolving Eq. (11) for  $\theta$ , one obtains

$$\cos^2 \theta = 1 - \left[ Q \frac{\Lambda_{L3} B(\phi_K)}{\Lambda_K B(\psi_1)} \right]^{1/2},$$

where the relations,  $\Lambda_{L3}/\Lambda_K < 1$  and  $Q \ll 1$ , are used. Substituting  $Q < 1.3 \times 10^{-4}$  and the values of  $\Lambda_{L3}/\Lambda_K$ ,  $B(\phi_K)$ , and  $B(\psi_1)$  in the above equation, we obtained  $\theta < 3.3^\circ$ . In addition, the NEET probability was given as  $P < 3.7 \times 10^{-3}$  from  $\theta$  and Eq. (4). Also,  $|E'| < 110$  eV and  $|\delta| < 7$  eV were obtained by using Eqs. (1) and (5), where the signs of  $E'$  and  $\delta$  were negative. It follows that the energy shift  $\delta$  can be neglected in analyzing "NEET-X".

Next, the influences of NEET on the decay process were evaluated for the case that the NEET probability was equal to the upper limit,  $P = 3.7 \times 10^{-3}$ . The results indicated that the intensity of the 103-keV  $\gamma$ -ray emitted in the NEET process, NEET- $\gamma$ , was less than 40% of the analyzed value of  $I_{\gamma}^{103}$ . This implies that the obtained upper limit of  $P$  is consistent with each measured  $\gamma$ -ray intensity. Furthermore, it was found that the influences of NEET on other  $\gamma$ -rays originating in the levels except the 103-keV one were negligibly small. Therefore, if the NEET probability is much smaller than  $3.7 \times 10^{-3}$ , the influences of NEET on the decay process should be almost negligible. In the consequence of this, we can conclude that,

as an upper limit of the NEET probability,  $P < 4 \times 10^{-3}$  was obtained by examining the Np K X-ray spectrum in the EC decay of  $^{237}\text{Pu}$ . It would be hard to determine the NEET probability by using a similar technique, even if it is improved.

Finally, the experimental electromagnetic interaction energy was compared with the theoretical one,  $E'_{theor}$ . The value of  $E'_{theor}$  can be calculated from Eq. (2). In the case that a common multipolarity is the electric component, as in the present case, the electric interaction between the orbital electron and the nucleus is considered to contribute mainly to this process. Then  $E'_{theor}$  will be evaluated for a possible interaction by assuming the Coulomb perturbation as  $H'$ ,

$$H' = -Ze^2 \left( \frac{1}{|\vec{r}_N - \vec{r}_e|} - \frac{1}{r_e} \right) \quad (12)$$

Here,  $\vec{r}_N$  is the position vector of the nucleus and  $\vec{r}_e$  that of the electron relevant to this process. By using Eq. (12), one can write Eq. (2) in the form

$$E'_{theor} = - \frac{4}{2\ell + 1} \alpha Z \langle r_N^\ell \rangle \langle r_e^{-(\ell+1)} \rangle mc^2 \quad (\ell \neq 0) \quad (13)$$

for  $E\ell$  transition.<sup>1)</sup> Here,  $\langle r_N^\ell \rangle$  and  $\langle r_e^{-(\ell+1)} \rangle$  are the off-diagonal matrix elements of  $r_N^\ell$  and  $r_e^{-(\ell+1)}$ , respectively,  $\alpha$  is the fine structure constant, and  $mc^2$  the electron rest energy. This equation is roughly expressed by

$$E'_{theor} = -3.41 \times 10^2 \frac{(2.27 \times 10^{-5})^{\ell} A^{\ell/3} Z^{\ell+2}}{(2\ell + 1) \bar{n}^{2(\ell+1)}} f \quad (14)$$

with the unit of eV.<sup>4)</sup> Here  $A$  and  $Z$  are the mass and the atomic numbers,  $\bar{n}$  is the average principal quantum number of two electron orbitals relevant to NEET, and  $f$  is the correction factor due to the collective character of the nuclear transition. In the case of  $^{237}\text{Np}$ , substituting  $A = 237$ ,  $Z = 93$ ,  $\bar{n} = 1.5$ , and  $\ell = 1$  in Eq. (14) yields  $E'_{theor} = -2.53 \times 10^3 f$  eV. From the values of  $E'_{theor}$  and the experimental  $E'$ , the correction factor  $f$  is found to be smaller than  $5 \times 10^{-2}$ . This suggests that the character of the nuclear transition may influence considerably the NEET process.

Here, we will consider the relation between NEET and the participant nuclear transition, and the property of the relevant nuclear transition. The transition probability is approximately proportional to  $|\langle r_N^{\ell} \rangle|^2$  for  $E\ell$  transition. From Eqs. (1), (4), and (13),  $P$  is also found to be proportional to  $|\langle r_N^{\ell} \rangle|^2$ . Therefore, it is considered that the NEET probability reflects the property of the nuclear transition. In general, the low-energy  $E1$  transitions in odd proton spheroidal nuclei in actinide region are highly retarded compared with the ordinary ones.<sup>19,20)</sup> In the ground level and the 59.5-keV level in  $^{237}\text{Np}$ , although there seem to be ample admixtures allowing the  $E1$  transition, the detailed  $E1$  calculations show that the contributions from

small parts of the wave function tend to cancel one another.<sup>20)</sup> Therefore, this transition is strictly forbidden. The hindrance factor,  $H_W$ , calculated relative to the theoretical single particle Weisskopf estimate is reported as

$$H_W = \frac{B(E1) [\text{exp.}]}{B(E1) [\text{Weisskopf}]} = 4.9 \times 10^{-6}$$

for the 59.5-keV  $\gamma$ -ray transition.<sup>19)</sup> The retardation of the relevant transition from the 103-keV level to the ground one is also considered to be the same orders of magnitude, because the 103-keV level belongs to the same rotational band as the 59.5-keV level as shown in Fig. 10. From the above discussion and the fact that the single particle estimate was employed in the calculation of  $\langle r_N^\ell \rangle$ , therefore, the NEET probability is presumed to be smaller by about five orders of magnitude than the theoretically estimated one. This supports that  $f$  is smaller than  $5 \times 10^{-2}$ , though a further discussion of  $f$  requires a more accurate calculation of  $\langle r_e^{-(\ell+1)} \rangle$ . Consequently, the NEET probability is predicted to be much smaller than  $4 \times 10^{-3}$ .

Recently, Saito et al.<sup>21)</sup> have detected NEET in  $^{237}\text{Np}$  by ionizing the K shell of Np artificially with photons and obtained  $P = (2.1 \pm 0.6) \times 10^{-4}$ , which is consistent with the present result.

If an excitation from one excited level by the NEET process is taken into account as well as that from the ground level,

one can expect the number of nuclides satisfying the NEET conditions to increase and possibly the NEET-nuclide with a large NEET probability to appear. The electron shell vacancy which can cooperate for NEET with the nucleus in the suitably excited state is often created in an ordinary decay process such as EC decay or internal conversion. Nevertheless, the detection of such NEET between the nuclear excited levels would also need an ingenious technique.

One of the authors (K.O.) would like to express his sincere thanks to the Takahashi Foundation for financial aid, to the Nishina Memorial Foundation for a grant, and to the Ministry of Education for a Grant-in-Aid.

## References

- 1) Morita M.: Prog. Theor. Phys., 49, 1574 (1973).
- 2) Otozai K., Arakawa R. and Morita M.: Prog. Theor. Phys., 50, 1771 (1973).
- 3) Otozai K., Arakawa R. and Saito T.: Nucl. Phys., A297, 97 (1978).
- 4) Otozai K.: Osaka University Laboratory of Nuclear Studies report OULNS 77-5 (1977).
- 5) Otozai K., Arakawa R., Morita M., Baba H., Hata K. and Suzuki T.: private communication (1976).
- 6) Hata K., Baba H., Umezawa H., Suzuki T. and Nozaki T.: Int. J. Appl. Radiat. Isot., 27, 713 (1976).
- 7) Natsume H., Umezawa H., Okashita H., Suzuki T., Sonobe T. and Usuda S.: J. Nucl. Sci. Technol., 9, 737 (1972).
- 8) Fioratti M. P. and Piermattei S. R.: Nucl. Instrum. Methods, 96, 605 (1971).
- 9) Baba H., Okashita H., Baba S., Suzuki T., Umezawa H. and Natsume H.: J. Nucl. Sci. Technol., 8, 703 (1971).
- 10) Baba H., Sekine T., Baba S. and Okashita H.: JAERI 1227 (1972).
- 11) Baba H.: JAERI-M 7017 (1977).
- 12) Cumming J. B.: National Academy of Sciences report NAS-NS 3107 (1962) p. 25.
- 13) Ellis Y. A.: Nucl. Data Sheets, 23, 71 (1978).

- 14) Lederer C. M. and Shirley V. S.: "Table of Isotopes" 7th ed.,  
Wiley, New York, (1978).
- 15) Currie L. A.: Anal. Chem., 40, 586 (1968).
- 16) Scofield J. H.: Atom. Data Nucl. Data Tables, 14, 121 (1974).
- 17) Ahmad I.: Z. Phys., A290, 1 (1979).
- 18) Fink R. W. and Rao P. V.: "Handbook of Spectroscopy" vol. 1.,  
ed. Robinson J. B., CRC press, Cleveland, (1974) p. 219.
- 19) Perdrisat C. F.: Rev. Mod. Phys., 38, 41 (1966).
- 20) Strominger D. and Rasmussen J. O.: Nucl. Phys., 3, 197 (1957).
- 21) Saito T., Shinohara A. and Otozai K.: Phys. Lett., 92B,  
293 (1980).



Table 1 Estimated values of the sum peaks

Peak	Energy	Intensities / cps	
	keV	Estimated*	Observed
$K_{\alpha 1} + (L_{\alpha 1} - \text{Ge})$	105.14	$3.8 \times 10^{-2}$	$3.5 \times 10^{-2}$
$K_{\alpha 2} + (L_{\beta 3} - \text{Ge})$			
$K_{\alpha 1} + (L_{\alpha 2} - \text{Ge})$	104.95	$2.2 \times 10^{-2}$	$2.0 \times 10^{-2}$
$K_{\alpha 2} + (L_{\beta 1} - \text{Ge})$			
$K_{\alpha 2} + (L_{\beta 2} - \text{Ge})$	104.04	$8.1 \times 10^{-4}$	$7.4 \times 10^{-4} \dagger$
$K_{\alpha 1} + (L_{\ell} - \text{Ge})$	103.08	$2.5 \times 10^{-3}$	$2.3 \times 10^{-3} \dagger$
$K_{\alpha 1} + M_{\alpha, \beta}$	$\sim 104$	$\sim 7 \times 10^{-3}$	$\sim 6 \times 10^{-3} \dagger$

\* These intensities are the estimates deduced from the observed intensities of  $K_{\alpha 1,2}$  X-rays and the theoretical intensities per decay of the sum peaks.

† These values were derived from the estimated intensity ratio and the observed intensities of the 105.14-keV and 104.95-keV sum peaks.

Table 2 Results of analysis

Peak	Symbol	Intensity / $10^{-3}$ cps
$K_{\alpha 1}$ X-ray	$I_{K\alpha 1}$	$11668.0 \pm 6.0$
NEET-X	$I_X^{103} \star$	$0.5 \pm 1.1$
103-keV peak	$I_{tot}^{103}$	$3.2 \pm 1.1$
NEET- $\gamma$ + Nuclear- $\gamma$ + (60-keV $\gamma$ + 43-keV $\gamma$ )	$I_{\gamma}^{103}$	$0.4 \pm 0.1$
$[K_{\alpha 1} + (L_{\ell} - \text{Ge})]$	$I_{sum}^{103}$	2.3

$$\star I_X^{103} = I_{tot}^{103} - (I_{\gamma}^{103} + I_{sum}^{103}).$$

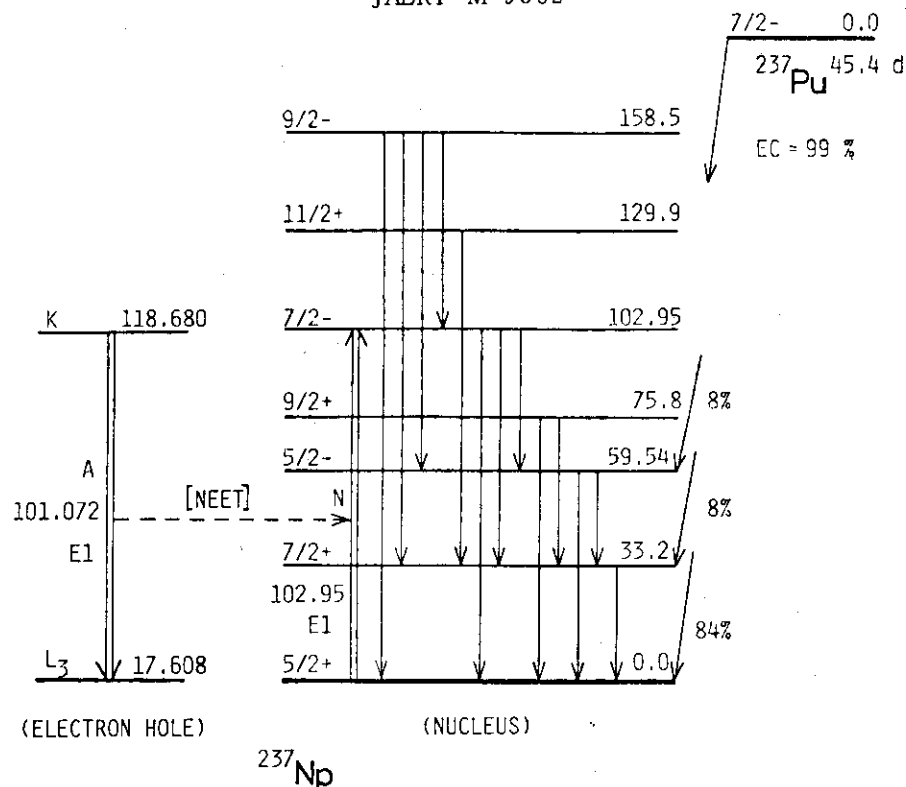


Fig.1 NEET DIAGRAM for  $^{237}\text{Pu} \rightarrow ^{237}\text{Np}$ . The decay scheme of  $^{237}\text{Pu}$  and the atomic levels relevant to NEET in  $^{237}\text{Np}$  are shown. Transitions *A* and *N* satisfy the NEET conditions when  $^{237}\text{Pu}$  decays to the ground state in  $^{237}\text{Np}$  by K-electron capture. These data were taken from Ref. <sup>14)</sup>

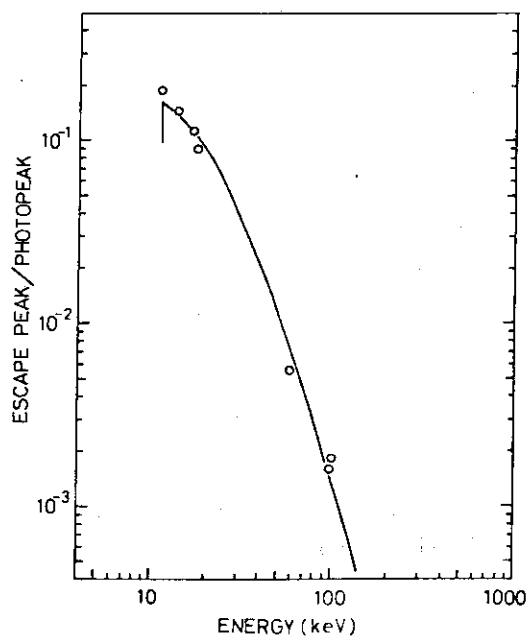
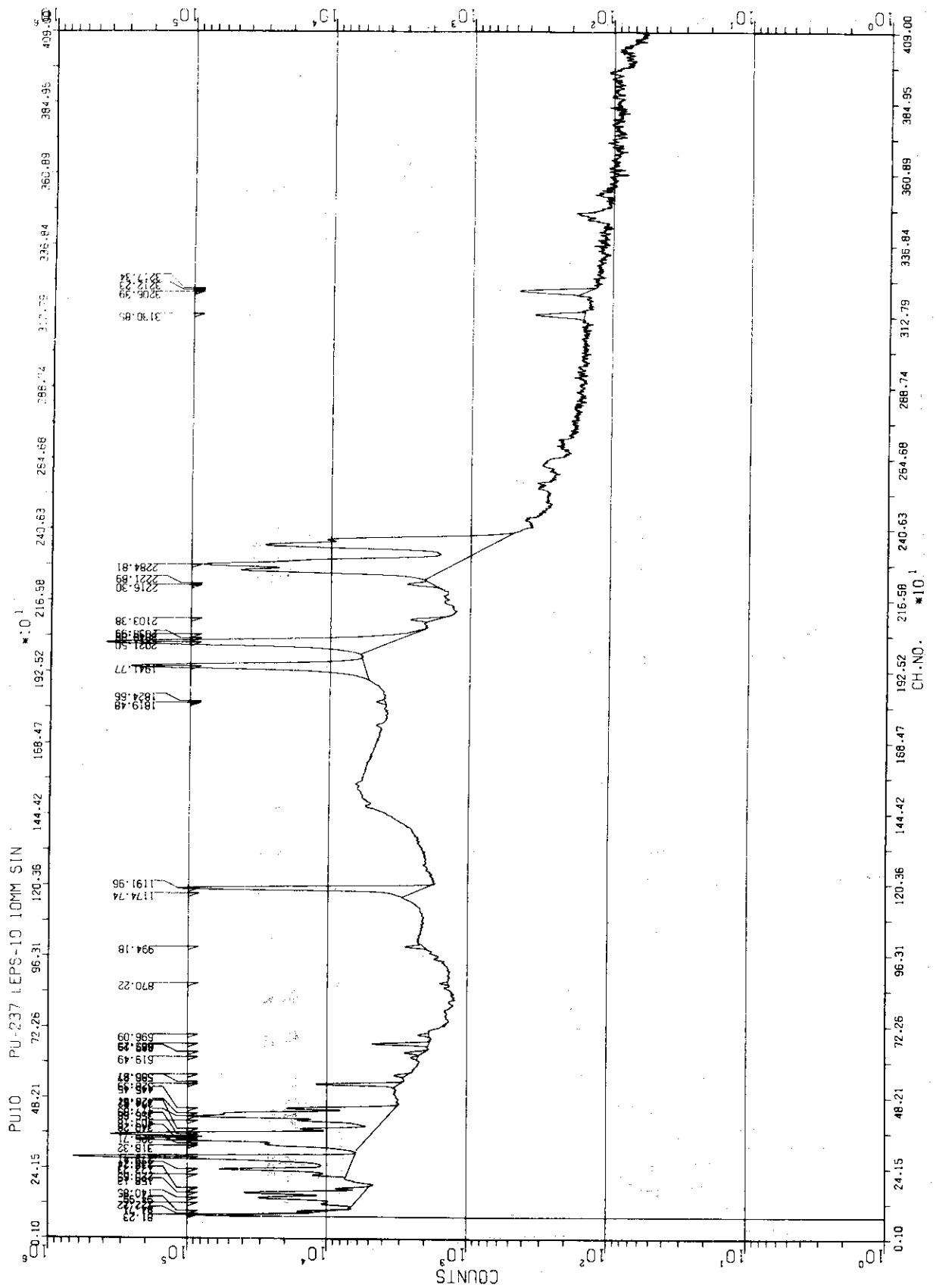
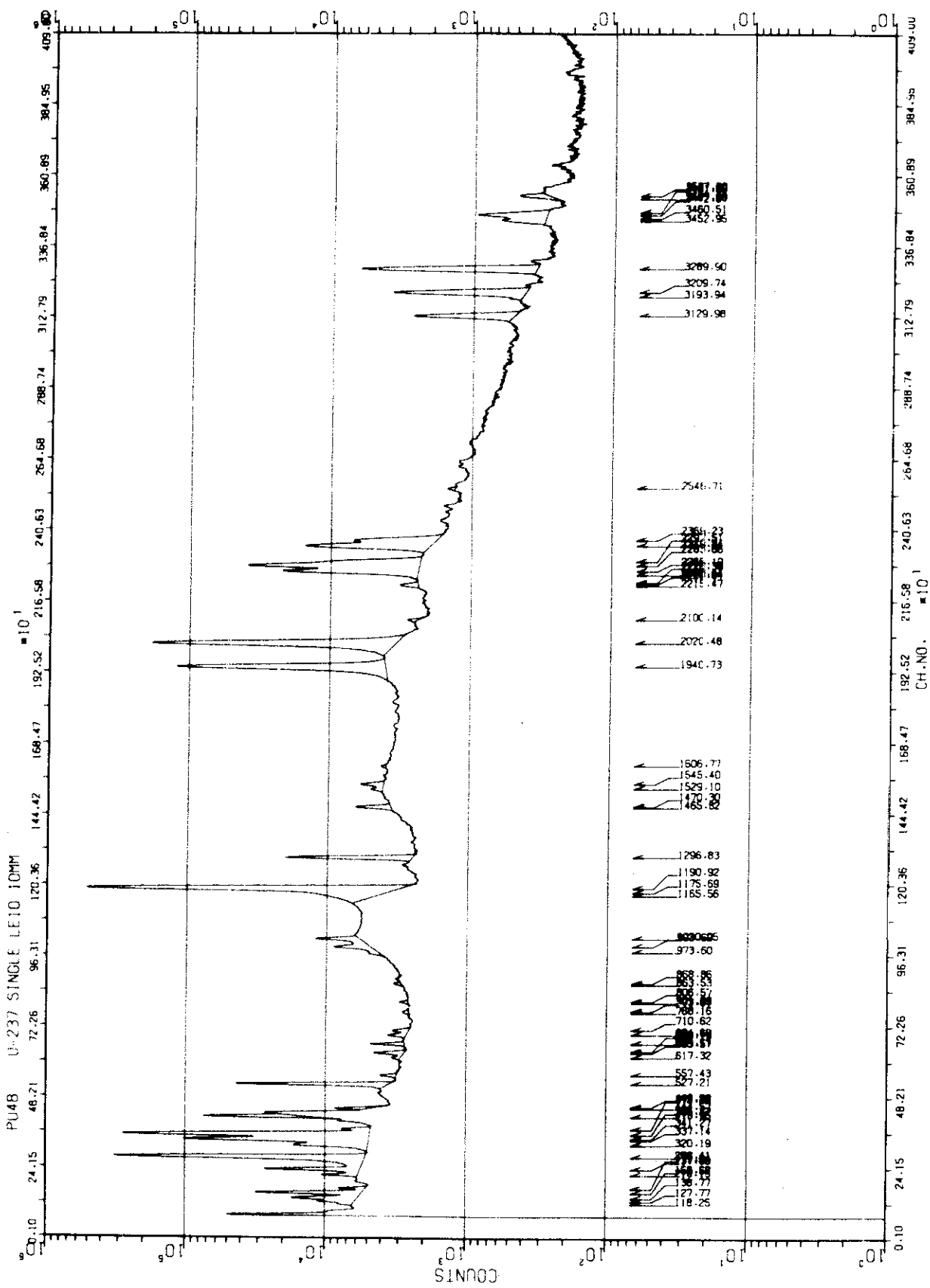


Fig.2 Ge  $K_{\alpha}$  X-ray escape ratio as a function of energy. The solid curve is that calculated by Fioratti and Piermattei. <sup>8)</sup>

Fig. 3 Photon spectrum of  $^{237}\text{Pu}$ .

Fig. 4 Photon spectrum of  $^{237}\text{U}$ .

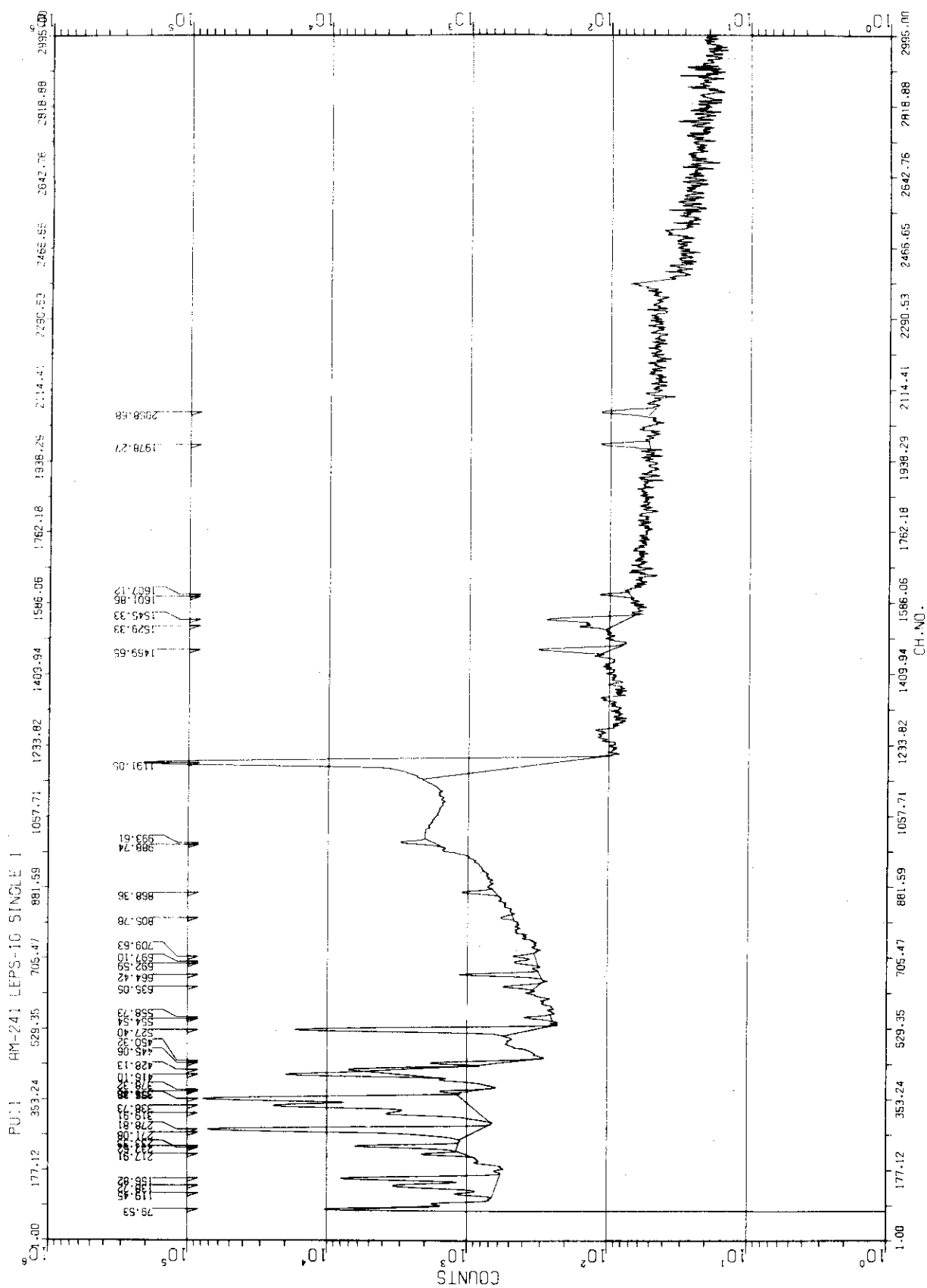


Fig. 5 Photon spectrum of  $^{241}\text{Am}$ .

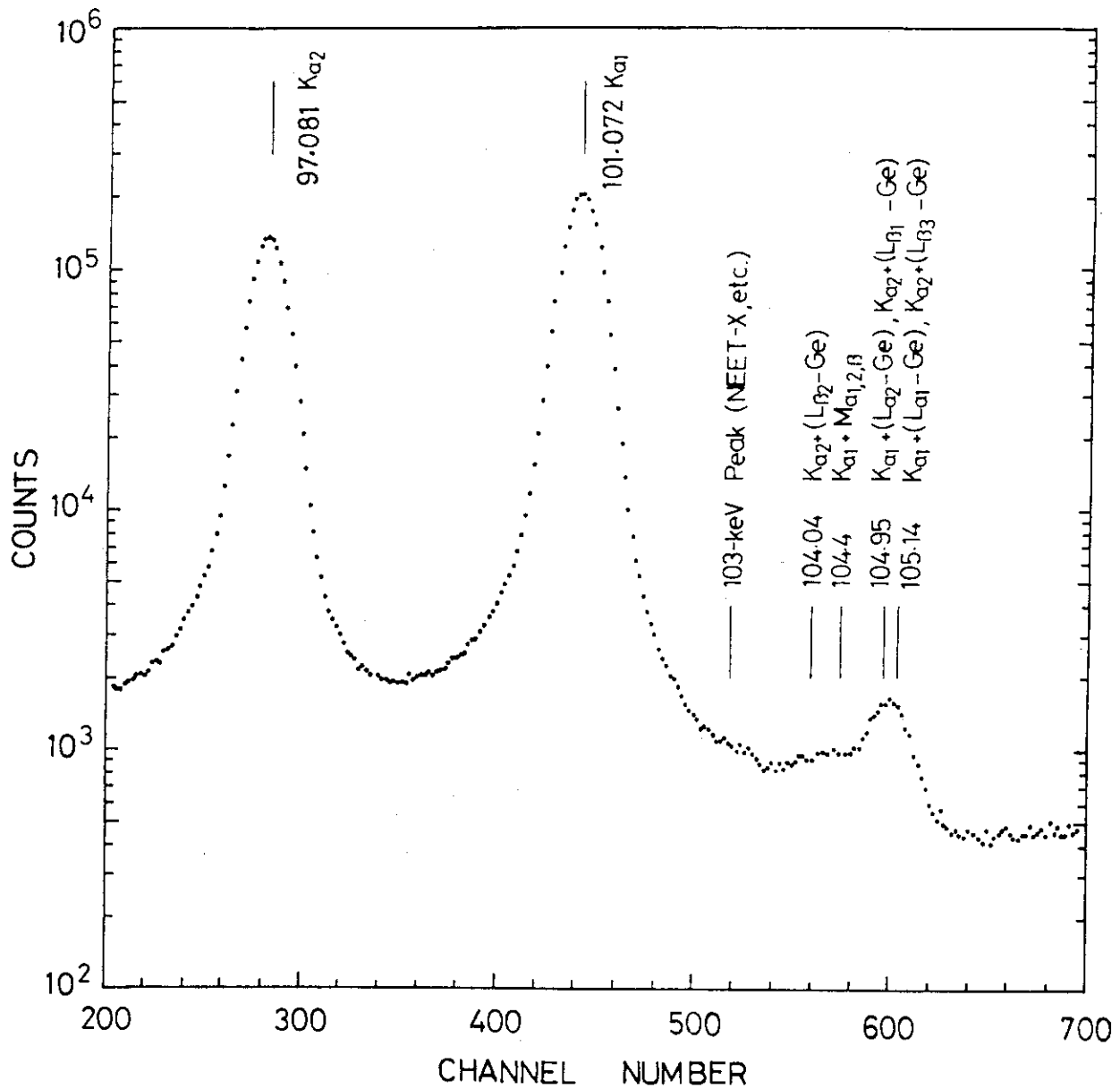


Fig.6 Typical photon spectrum in the neighborhood of  $K_{\alpha}$  X-rays of Np in the EC decay of  $^{237}\text{Pu}$ . For example,  $(L_{\alpha 1} - \text{Ge})$  refers to the Ge-escape peak of  $L_{\alpha 1}$  X-ray and  $K_{\alpha 1} + (L_{\alpha 1} - \text{Ge})$  refers to the sum peak of  $K_{\alpha 1}$  X-ray and  $(L_{\alpha 1} - \text{Ge})$  peak. The "NEET-X" in question lies at 103 keV.

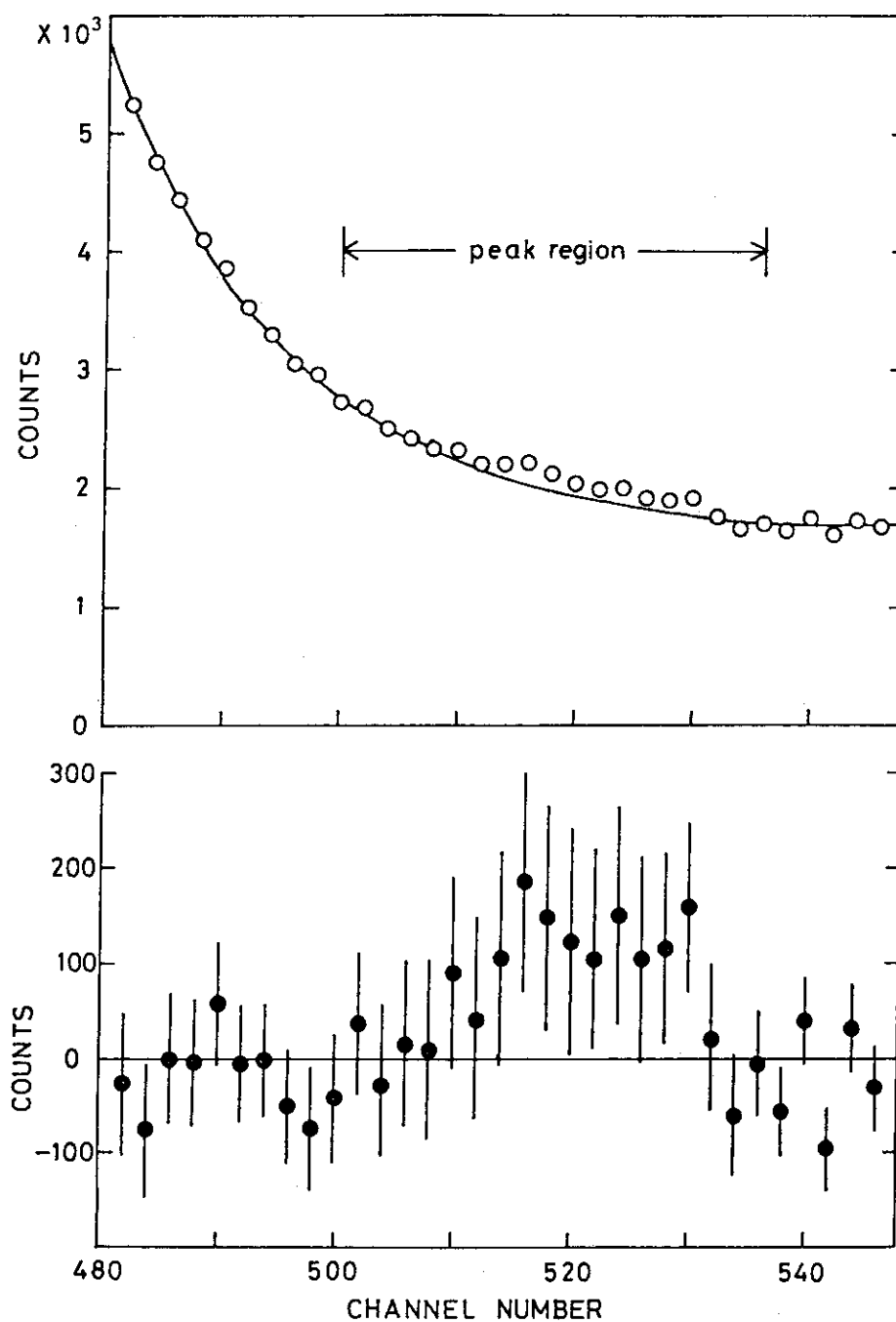


Fig.7 Two-channel-sum spectrum of the 103-keV region in  $^{237}\text{Np}$  and the result of analysis for the 103-keV peak. This spectrum was obtained from the measurement with the acquisition time of 6700 min. the solid curve in the upper figure is the fifth-order polynomial fitted to the observed counts except the region of the 103-keV peak. The result yielded by subtracting the baseline built by interpolation of the measured outskirts with the polynomial is also shown in the lower figure.

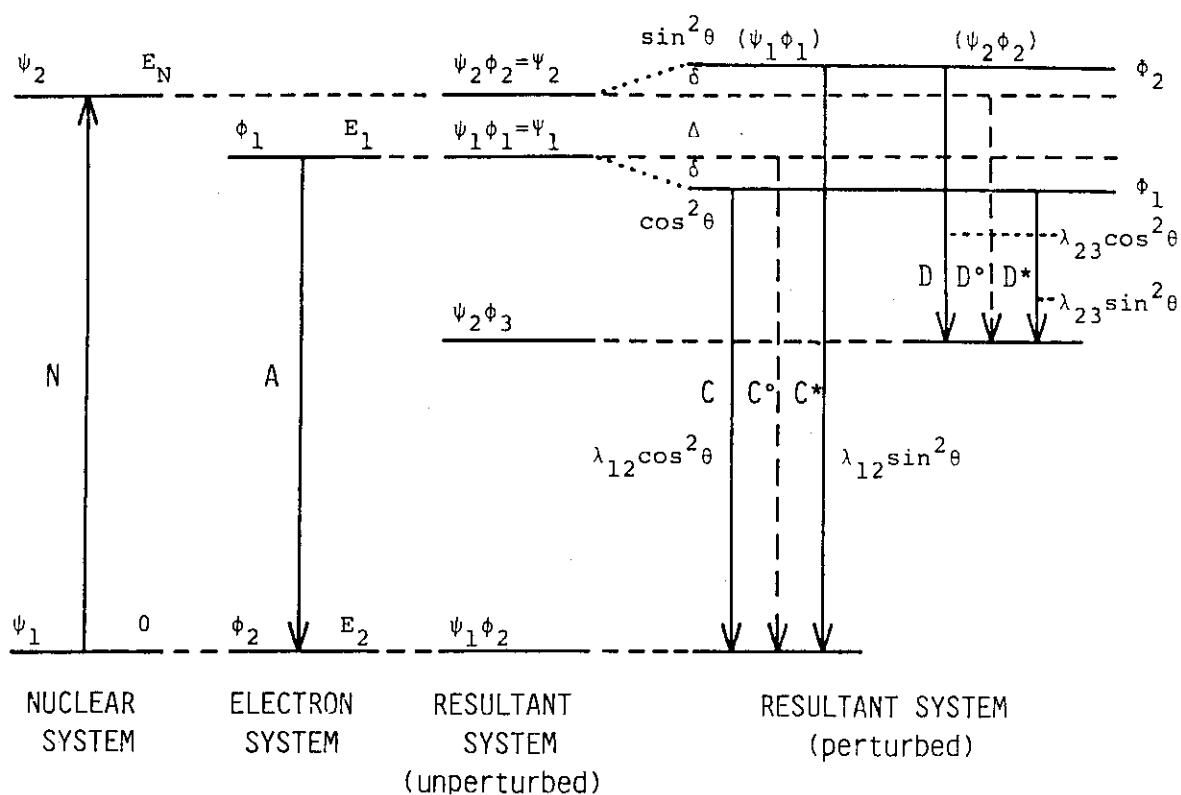


Fig. 8 Principle of NEET

9/2- 158.5

11/2+ 129.9

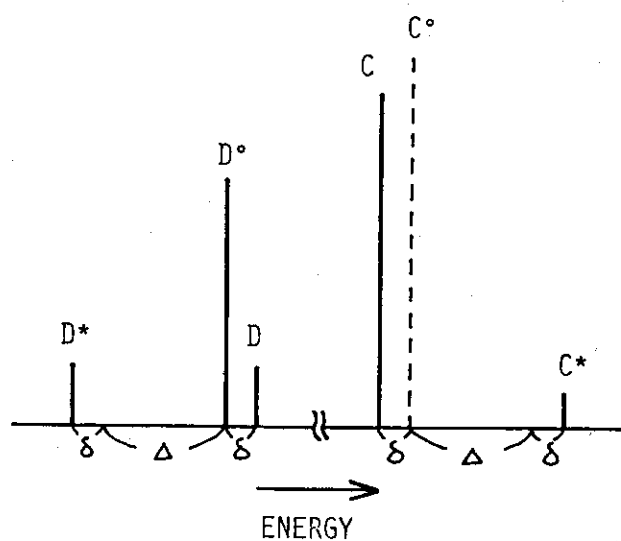
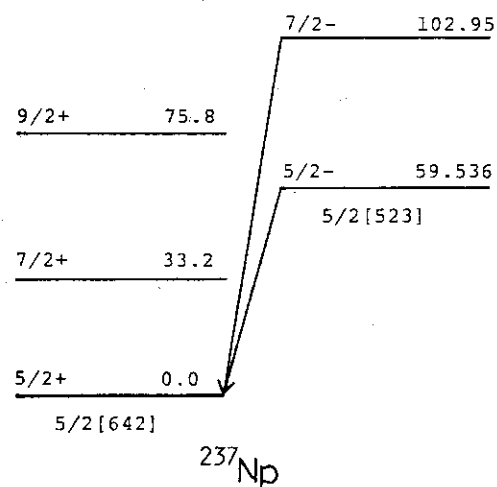


Fig.9 View of the satellite lines predicted by the NEET theory.

Fig.10 Rotational bands of  $^{237}\text{Np}$  nucleus. Both transitions from a 5/2-level to the ground one and from a 7/2-level to the ground one, which are shown with arrows, are considered to be retarded similarly.